ACS OMEGA

http://pubs.acs.org/journal/acsodf

Article

Probing the Molecular Assembly of a Metabolizer Drug with β-Cyclodextrin and Its Binding with CT-DNA in Augmenting Antibacterial Activity and Photostability by Physicochemical and Computational Methodologies

Modhusudan Mondal, Shatarupa Basak, Debadrita Roy, Md Salman Haydar, Subhankar Choudhury, Biswajit Ghosh, Narendra Nath Ghosh, Ankita Dutta, Palash Mandal, Kanak Roy, Anoop Kumar, and Mahendra Nath Roy*

Cite This: *ACS Omega* 2022, 7, 26211−26225

Read Online

ACCESS | Metrics & More | Article Recommendations | Supporting Information

ABSTRACT: The assembly of an inclusion complex in an aqueous medium using a metabolizer drug (dyphylline) as guest and β-cyclodextrin as host has been established, which is extremely appropriate for a variety of applications in modern biomedical sciences. The formation of the inclusion complex is established by ^{1}H NMR, and surface tension and conductivity measurements demonstrate that the inclusion complex was produced with 1:1 stoichiometry. The thermodynamic parameters based on density, viscosity, and refractive index measurements were used to determine the nature of the complex. This research also forecasts how dyphylline will release in the presence of CT-DNA without any chemical modifications. The produced insertion complex (IC) has a higher photostability due to the drug dyphylline being protected by β-CD. The antibacterial activity of dyphylline greatly improved after complexation and exhibited higher toxicity against Gram-negative (highest against *Escherichia coli*) in comparison to Gram-positive bacteria. The encapsulation mode of the dyphylline molecule into the cavity of the β-CD was also investigated using DFT to confirm preliminary results.

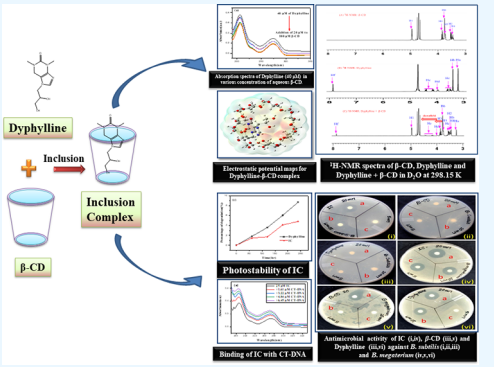

1. INTRODUCTION

When A. Villiers originally described cyclodextrins (CDs) in 1891, they were mentioned as "Cellulosine" are the cyclic oligosaccharide family members that include 6 (α-CD), 7 (β-CD), and 8 (γ-CD) glucopyranose units linked by α-(1−4) links.[1−3] The ring structure of CDs is torus-shaped, with polar hydrophilic rims and a moderately hydrophobic core hollow.[4] Owing to their unusual structure, they can form host−guest inclusion or insertion complexes (ICs) with different hydrophobic guests such as medicines, amino acids, dyes, ionic liquids, etc. The nonpolar component of the incoming guest molecule is accommodated in their hydrophobic hollow, and the polar portion of the visitor molecule is stabilized by the polar rims.[5,6] This explains the current fascination with CDs for the regulated release of bioactive compounds, drugs, food flavors, deodorizers, paint components, and other similar substances, as well as the chemical-free removal of dangerous elements, waste products, and pollutants.[7]

7-(2,3-Dihydroxypropyl)theophylline, dyphylline for short, is one of the most widely approved drugs used in therapy for respiratory illnesses such as asthma, emphysema, cardiac dyspnea, and chronic obstructive pulmonary disease (COPD). It belongs to the xanthine derivative family. However, because it is inexpensive and widely available in developing nations, dyphylline is being phased out as the first-line treatment for persons with asthma and COPD. Low-dose dyphylline provides anti-inflammatory and immunological modulatory effects in asthma and COPD according to a growing body of evidence, and as a result, dyphylline has sparked a lot of interest and importance.[8,9] Dyphylline rapid metabolizers, which are commonly started in children and adults who smoke, may require a longer, more regular interval than once-a-day dosing, and higher fluctuations in theophylline levels should be expected.[10] The main toxicity of THP intoxication varies contingent on the type of overdose.[11]

In this work, we attempted to determine the nature of the formation of IC of β-CD with dyphylline in 0.001, 0.003, and 0.005 mass fractions of β-CD in an aqueous medium. The

Received: March 29, 2022
Accepted: June 30, 2022
Published: July 19, 2022

incorporation of dyphylline into aqueous β-CD has been investigated in this study, with an emphasis on the encapsulation of dyphylline into the cavity of β-CD, in addition to their creation, stabilization, carrying, and controlled release without chemical modification utilizing several dependable methods. To communicate a quantitative idea about the encapsulation of the above medicine while complexed with CDs, thermodynamic characteristics have been analyzed as well.[12] Density, viscosity, and refractive index measurements were used to investigate the nature of the IC and their interactions, with various groups of the dyphylline contributing to the limiting apparent molar volume and viscosity B-coefficient. Additionally, conductance and surface tension data support the data inclusion behavior. To confirm the 1:1 inclusion phenomenon, Job's plot was performed using UV−visible spectroscopy, and the binding constants were estimated using the Benesi−Hildebrand method. The binding behavior and the nature of interaction with CT-DNA of the pure drug and the presence of β-CD were also established by estimating their binding constant and Gibbs free energy values. Thus, the goal of this kind of study is to develop controlled-release systems to reduce dosing frequency, improve therapeutic effectiveness by lowering the required dose, provide a consistent drug delivery method, and enable the intended application in the pharmaceutical science to be carried out.

To establish the pharmacological benefits of dyphylline IC, the antibacterial activity of dyphylline encapsulation was tested against several pathogenic bacteria including Gram-positive and Gram-negative bacteria. This specific antibacterial study was chosen as bacterial resistance to various antimicrobial agents (due to prolonged administration of antibiotics) is a rising problem for all hosts and of all ages. Finally, density functional theory calculations were used to evaluate optimal geometries, adsorption energies, noncovalent interaction (NCI), and electrostatic potential energy maps to connect with experimental results (ESP).

2. EXPERIMENTAL SECTION

2.1. Materials' Details. Dyphylline and β-CD were acquired from TCI in India and Sigma-Aldrich in Germany, respectively. Table S1 lists the CAS Registry Nos., suppliers, and mass fractions. All of the compounds are used without being purified further.

2.2. Methods and Apparatus. The solubility of dyphylline and β-CD in triply distilled water and degassed water was thoroughly tested before the start of the experiment, and it was noticed that the selected drug was freely soluble in all proportions of the β-CD solution. All of the β-CD and dyphylline stock solutions were prepared by mass (using a Shimadzu electronic balance with ±0.01 mg uncertainty), and the experimental solutions were obtained by mass dilution at 298.15 K. The densities of the solutions were used to convert molarity to molality.

The densities (ρ) of the experimental solutions were measured using a vibrating-tube density meter (DMA 4500 M). Before each series of density measurements, the DMA was calibrated with triply distilled water and dry air at atmospheric pressure, as indicated in the user handbook, at the experimental temperature ranges.

The viscosity measurements were performed in a Brookfield digital viscometer (USA, with spindle number 42 and uncertainty ±0.003 mPa·s) with water flowing from a Riviera Glass high-precision water thermostat (±0.01 K) (Mumbai, India).

A digital refractometer from Mettler Toledo (India) with an uncertainty of ±0.0002 was used to analyze the refractive indices of experimental solutions after rectifying it twice with distilled water and calibrating it after every few measurements.

The surface tension and conductance studies were carried out at the examined temperature utilizing a Tensiometer (K9, KRUSS; Germany) and Systronics 308 digital conductivity meter with an accuracy of ±0.01 mN/m and ±0.01%, respectively.

A JASCO V-530 UV−vis spectrophotometer and Bruker AVANCE (400 MHz) were used to obtain UV−visible spectra and NMR spectra. For the ^{1}H NMR using residual protonated solvent (HDO) signals as an internal standard (D_2O: −4.79 ppm), signals are expressed as δ-values in ppm. Chemical shifts are used to report data. All the UV−visible related solutions are prepared in an aqueous medium.

2.3. Computational Details. In the present work, all theoretical calculations were performed by employing density functional theory (DFT) using the Gaussian 16 program.[13] Ground state geometry optimizations of the dyphylline, β-CD, and dyphylline−β-CD IC were carried out at the M06-2X/6-31+G (d) level of theory. Hybrid functionals like M06-2X offer reliable and precisely noncovalently bonded interaction energies for hydrogen-bonded and $\pi-\pi$ stacked systems.[14] In the due course of ground state optimization, solvent effects (water) were introduced by applying the polarizable continuum model (PCM).[15] To inspect whether the optimized geometry exists in the minima on the potential energy surfaces, vibration frequency analysis (no imaginary frequency) was performed at the same level of theory. Various weak interactions like H-bonding, van der Waals interactions, and steric interactions were visualized by reduced density gradient (RDG) using the Multiwfn 3.7 suite.[16] To account for the extent of charge-transfer interactions in dyphylline−β-CD IC in an aqueous medium, molecular electrostatic potential (MESP) maps were generated at the same level of theory. Adsorption energies (ΔE_{ads}) of the inclusion complex were calculated using the following formula:

$$\Delta E_{ads} = E_{\text{dyphylline}-\beta-\text{CD}} - E_{\text{dyphylline}} - E_{\beta-\text{CD}} \quad (1)$$

where $E_{\text{dyphylline}-\beta\text{-CD}}$, $E_{\text{dyphylline}}$, and $E_{\beta\text{-CD}}$ are the total energy of the geometry optimized complexes, free dyphylline, and β-CD molecules, respectively.

2.4. Antibacterial Study. The antimicrobial activity of the synthesized inclusion complex (IC) in comparison to the host (β-CD) and guest (dyphylline) was assessed against two Gram-negative and three Gram-positive bacterial strains following the disk diffusion method.[17] Gram-positive facultative anaerobic cocci *Staphylococcus aureus* ATCC 11,632 and aerobic or facultative endospore-forming *Bacillus megaterium* ATCC 14,581 and *Bacillus subtilis* ATCC 11,774, along with Gram-negative *Escherichia coli* ATCC 11,229 and *Salmonella typhimurium* ATCC 25,241, were chosen for the study. To get fresh and viable cells for the experiment, the studied microbes were grown in a nutrient broth for 6−8 h. From the nutrient broth, 200 μL of the actively growing test organism was added to the nutrient agar plate and, after uniform mixing, allowed to solidify. Paper disks soaked with three different (20, 10, and 5 mM) concentrations of tested samples were placed on the agar surface. The bactericidal activity of the studied samples was

https://doi.org/10.1021/acsomega.2c01902
ACS Omega 2022, 7, 26211−26225

evaluated in terms of the zone of inhibition (measured using a millimeter scale around the disk).

2.5. MTT Assay. ACHN (human malignant kidney cell line) (the ACHN cell line was procured from NCCS, Pune, India) was grown in a 96-well microtiter plate at 37 °C in the presence of 5% CO_2 at a density of 4×10^3 cells/well in 100 μL of DMEM (Dulbecco's modified Eagle MEDIUM) Ham F-12 growth medium. After a 24 h incubation period, medicines dyphylline and its IC were introduced in triplicate to each well at various doses (50, 100, 150, 200, 250, 300, 350, 400, 450, and 500 μM). Under the same experimental conditions, the microtiter plate was incubated again. After discarding the culture media, the treated plate was removed from the incubator, and 10 μL (5 mg/mL) of the MTT powder diluted in 1× PBS was added to each well. After that, the plate was left in the same state for 3 h. Finally, each well containing the MTT solution received 50 μL of isopropanol, a formazan solubilizer, which was agitated for about 5 min. Finally, an ELISA reader was used to measure absorbance at 620 nm.

The proportion of cell toxicity was computed as $\{(X - Y)/X \times 100\}$, where X represents the mean optical density of untreated cells and Y represents the mean optical density of treated cells at various drug dosages.

2.6. Statistical Analysis Method. All the experimental data were taken three times; i.e., all tests were done in triplicate using the said instruments discussed in the Methods and Apparatus section, and the instruments were calibrated with standard protocols to determine the density, viscosity, refractive index, etc. The mean values were listed in tables, and the standard deviations (standard uncertainties) from the mean were written as footnotes in tables containing raw data.

3. RESULTS AND DISCUSSION

3.1. Conductivity Study Illustrates the Inclusion Process and Their Stoichiometric Ratio. The conductivity (κ) analysis not only validates the creation of a supramolecular host−guest IC but also provides information on the molecular assembly's stoichiometric ratio.[18] We evaluated the conductivity of the examined dyphylline aqueous solutions with an initial concentration of 10 mM and subsequent addition of β-CD at 298.15 K (Table S2). It has been discovered that as the concentration of β-CD increases, the conductivity of dyphylline decreases on a regular basis (Figure S1 and Table S2). This finding corresponds to the creation of IC.[19] The insertion of the guest drug molecule into the cavity of the β-CD molecule reduces the mobility of the latter, resulting in a drop in the number of free ions per unit volume and a reduction in the solution's conductivity.[20] The curve (Figure S1 and Tables S2) reveals a similar result, with a distinct break indicating the creation of the dyphylline−β-CD inclusion with a 1:1 stoichiometry. Table 1 shows the values and the associated concentrations of dyphylline and β-CD at the breaking point.

Table 1. At 298.15 K, Conductance and Surface Tension Values at the Break Point and the Corresponding CD and Dyphylline Concentrations

conductance			
system	conc. of dyphylline (mM)	conc. of β-CD (mM)	conductance (μS·m^{-1})
dyphylline + β-CD	5.13	4.87	10.62
Surface tension			
	conc. of dyphylline (mM)	conc. of β-CD (mM)	surface tension (mN/m)
dyphylline + β-CD	4.48	5.52	66.64

3.2. Surface Tension to Prove Inclusion Phenomena and Stoichiometric Ratio. The surface tension (γ) of the examined drug molecule (dyphylline) with β-CD is also an essential measure that suggests the creation of an IC.[21] With the addition of β-CD, the surface tension of water does not change significantly, indicating that CD is a surface inactive molecule.[22] The taken drug molecule's concentration was determined in our current study by raising the concentration of β-CD at 298.15 K (Table S3). With the addition of β-CD, the values for the dyphylline drug molecule significantly rose, most likely because the surface-active drug molecule was removed from the surface solution; i.e., the hydrophobic portion of the dyphylline molecule entered the hydrophobic hollow forming the host−guest IC.[23] The curve shows a single break point, and after that point, the γ value becomes approximately steady, which confirms the formation of a 1:1 inclusion complex (Figure 1 and Table 1). More breakdown points in the curve would indicate the formation of IC with 1:2, 2:1, etc., stoichiometry (Scheme 3).[24] Hence, this study proves the development of 1:1 IC.

3.3. Ultraviolet Spectroscopy: Job Plot. UV−visible spectroscopy is another important approach for learning about IC in aqueous systems. The stoichiometry of the host−guest relationship was determined using Job's approach, often known as the continuous variation method.[25] The drug molecule, dyphylline, and β-CD solutions were mixed at different concentration ratios R = [dyphylline]/([dyphylline] + [β-CD]), while the total concentration [dyphylline] + [β-CD] remained constant and the dyphylline mole fraction varied between 0 and 1 (Table S4). We obtained the Job's figure by plotting $\Delta A \times R$ versus R, where ΔA represents the absorbance difference between dyphylline without and with β-CD and R = [dyphylline]/[dyphylline] + [β-CD]). The solutions' absorbance values were measured at λ_{max} = 206 nm for dyphylline at 298.15 K (Figure 2b). The R value at the largest deviation point of the plot can be used to determine the stoichiometry of the inclusion complex (R = 0.5 for the 1:1 complex, R = 0.33 for the 1:2 complex, and R = 0.66 for the 2:1 complex).[26] The greatest deviation points in the curve corresponding to R in our analysis is 0.5083 (Figure 2a), indicating that the IC has a molar ratio of 1:1.[12]

3.4. Ultraviolet Spectroscopy: Association Constant. On the basis of change in molar absorptivity of dyphylline when complexed into the β-CD molecule, the association constant K_a for the dyphylline−β-CD system was determined using the UV−visible spectroscopic technique.[24] This is due to a change in the polarity of the dyphylline's surroundings when it moves from the polar aqueous environment to the nonpolar chamber of the β-CD (Figure S2). The change in absorption intensity of dyphylline (λ_{max} = 206 nm) as a function of β-CD concentration was investigated to determine the value of K_a (Table S5). The Benesi−Hildebrand approach was used to generate the double reciprocal plot (Figure S3) for the 1:1 host−guest (H−G) complex following

$$\frac{1}{\Delta A} = \frac{1}{\Delta\varepsilon[G]K_a}\cdot\frac{1}{[H]} + \frac{1}{\Delta\varepsilon[G]} \quad (2)$$

https://doi.org/10.1021/acsomega.2c01902
ACS Omega 2022, 7, 26211−26225

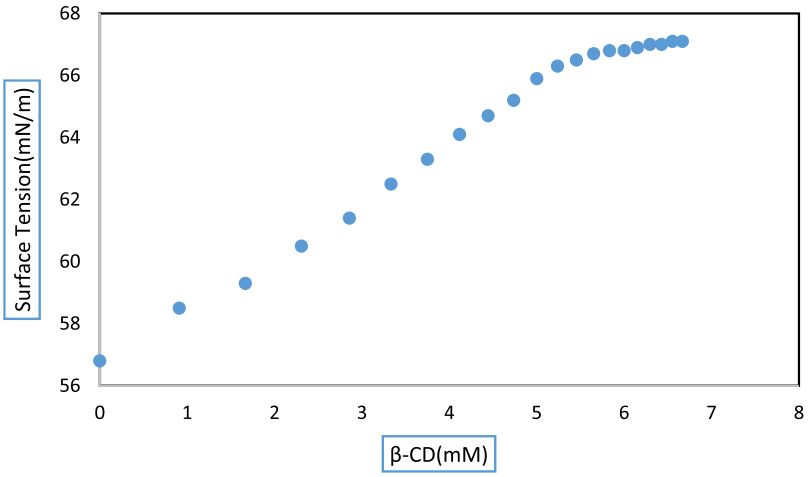

Figure 1. Variation of surface tension of the aqueous dyphylline–β-CD system at 298.15 K.

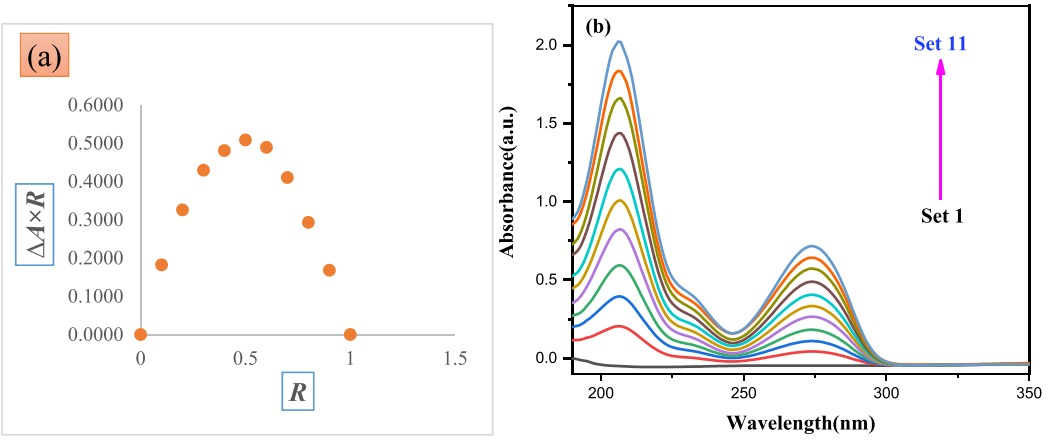

Figure 2. (a) Job plot and (b) spectra of aqueous dyphylline–β-CD system at λ_{max} = 206 nm at 298.15 K.

The intercept is divided by the slope of the straight line of the double reciprocal plot to get the value of the analyzed system's association constant (Table 2).[27]

Table 2. Values of the Association Constant (K_a) and Free Energy Change (ΔG^0) of the Dyphylline–β-CD

complex systems	T (K)[a]	K_a (M^{-1})	ΔG^0 (kJ mol^{-1})
dyphylline–β-CD	298.15	2.93×10^3	−19.35

[a]Standard uncertainty in temperature is u (T) = ±0.01 K

We can easily get the thermodynamic parameter from the association constant derived from the previous equation using the following free-energy-related equation:

$$\Delta G^0 = -RT \ln K_a \quad (3)$$

Using the foregoing eq 3, the value of ΔG^0 was found to be negative (Table 2), showing that the inclusion process occurs spontaneously.[28,29]

3.5. ^{1}H NMR Study. The interaction between dyphylline and β-CD causes the chemical shift of the various protons of the guest (dyphylline) and host (β-CD) molecules in the NMR spectra.[24] The H3 and H5 hydrogens are placed inside the cavity of the three-dimensional structure of β-CD, with H3 near the larger rim and H5 near the narrower rim; the remaining protons H1, H2, and H4 are present outside the cavity of β-CD (Schemes 1 and 2).[12,30] The chemical shift points (δ) for H3 and H5 are higher (downfield shift) in the complex than in pure β-CD according to NMR spectra (Figure 3 and Figure S4c). The amount of downfield shift for H5 is less than that of H3 (Table 3), which suggests that the guest molecule enters the cavity of β-CD through the wider rim side.[31,32] A considerable change in the chemical shift has been observed for the protons Hc, Hd, and He. The only aromatic proton of dyphylline, i.e., Hf proton, got shifted toward downfield in the complex, which resulted in a chemical shift difference of 0.005 ppm with respect to the pure one (Figure S4). Thus, differentiating the spectrum of the complex compared to the pure one proved that the hydrophobic portion of dyphylline is inserted from the wider rim to form IC.

3.6. SEM Analysis. The surface character, morphology, and particle size of solid sample entities can all be examined using scanning electron microscopy. This advances our knowledge of how ICs between the dyphylline and β-CD molecules form.[24,27] The surface morphology of pure dyphylline, β-CD, and the ICs that result is shown in Figure 4. Individual pure β-CDs may be seen on SEM images due to their cubic type size or polyhedral crystal-like structure, but dyphylline has a structure that is comparable to that of a long rectangular irregular shape type crystal and can be readily seen due to its odd shape. The surface shape of the molecule changes to a threadlike structure when dyphylline and β-CD (Figure 4c) are

https://doi.org/10.1021/acsomega.2c01902
ACS Omega 2022, 7, 26211−26225

Scheme 1. Molecular Structures of Beta-Cyclodextrin and Dyphylline

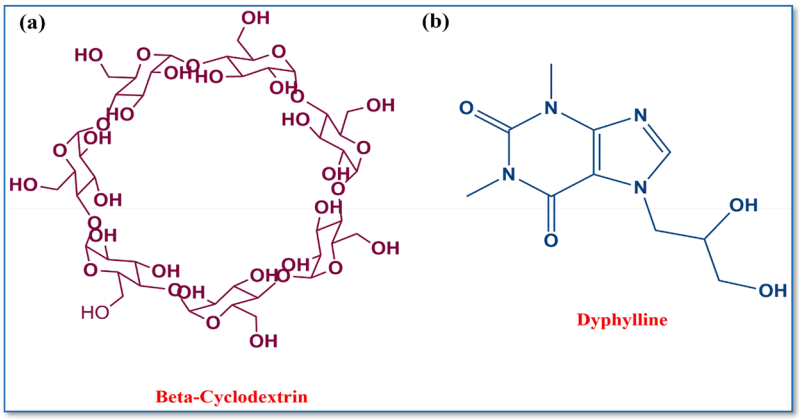

Scheme 2. Structures of β-CD and Dyphylline

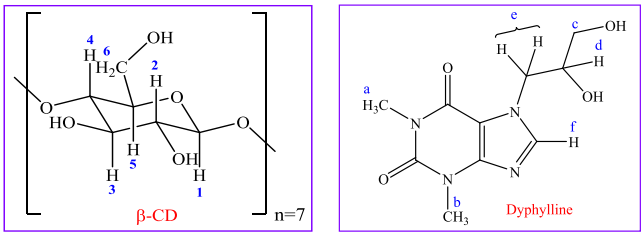

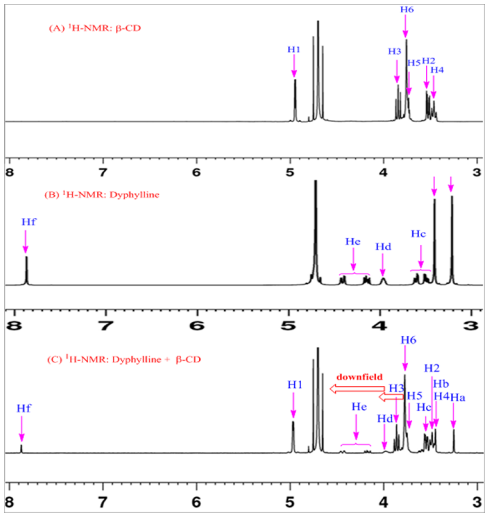

Figure 3. ^{1}H NMR spectra of pure host (β-CD), guest (dyphylline), and IC. Panel B is reprinted with permission from ref 24. Copyright 2022 Elsevier.

complexed, and they are found to have uneven shaped crystal units with bulky dimensions. The unusual surface form could be attributed to the IC's construction. As a result, the completely distinct surface form of the IC may enhance the other experimental findings.

3.7. Structural Influence of Cyclodextrin. The polar rims of the β-CD molecule provide an ideal environment for linking with the host molecule's polar side and thus stabilizing the IC. The hydrophobic cavity and hydrophilic rims of the β-CD molecule make it an ideal host molecule for interacting with the hydrophobic portion of the studied guest molecule inside the cavity. The diameter of the cavity in the β-CD is 6.0−6.5 mm (Scheme 3). During the formation of the IC, no

Table 3. Change in Chemical Shifts (ppm) of Different Protons of Dyphylline and β-CD When Complexed with Each Other at 298.15 K

	ppm (D_2O)			
H protons	$\delta_{dyphylline}$	$\delta_{\beta\text{-CD}}$	$\delta_{complex}$	$\Delta\delta$ (difference) (ppm)
Ha	3.207		3.248	0.041
Hb	3.398		3.504	0.106
Hc	3.543		3.603	0.060
Hd	3.962		3.967	0.007
He	4.403		4.439	0.036
He′	4.134		4.170	0.036
Hf	7.865		7.870	0.005
H-1		4.945	4.965	0.020
H-2		3.523	3.549	0.026
H-3		3.842	3.860	0.018
H-4		3.460	3.451	0.009
H-5		3.740	3.749	0.009
H-6		3.754	3.773	0.019

covalent bonds are formed or disrupted.[24,33] The key driving factor for the formation of IC is the replacement of polar water molecules from the hydrophobic cavity of the β-CD by the hydrophobic moiety of dyphylline, which is energetically unfavorable. This is more energetically advantageous. The surface tension, Job's plot, conductivity, and UV−visible spectroscopy tests all support the 1:1 stoichiometry of the IC.

3.8. Apparent Molar Volume. Volumetric parameters such as apparent molar volume (ϕ_V) and limiting apparent molar volume (ϕ_V^0) are important tools for understanding molecular interactions in solutions.[34] The ϕ_V is equal to the geometric volume of the central solute molecule plus variations in the solvent volume owing to interaction with the solute as it moves about the co-sphere. As a result, ϕ_V was computed using the appropriate equation from solution densities,[35] and the results are presented in Tables S6−S12.

$$\phi_V = M/\rho - (\rho - \rho_0)/m\rho\rho_0 \quad (4)$$

where M denotes the molar mass of the solute present and m, ρ, and ρ_0 are the molality and density of the solution (dyphylline in aqueous β-CD) and aqueous β-CD, respectively.

All of the experimental systems had positive ϕ_V values, indicating that there are strong solute−solvent interactions present. At a constant temperature, ϕ_V decreases with increasing dyphylline concentration (molality, m) in the same mass fraction of aqueous β-CD. It is also clear that ϕ_V

https://doi.org/10.1021/acsomega.2c01902
ACS Omega 2022, 7, 26211−26225

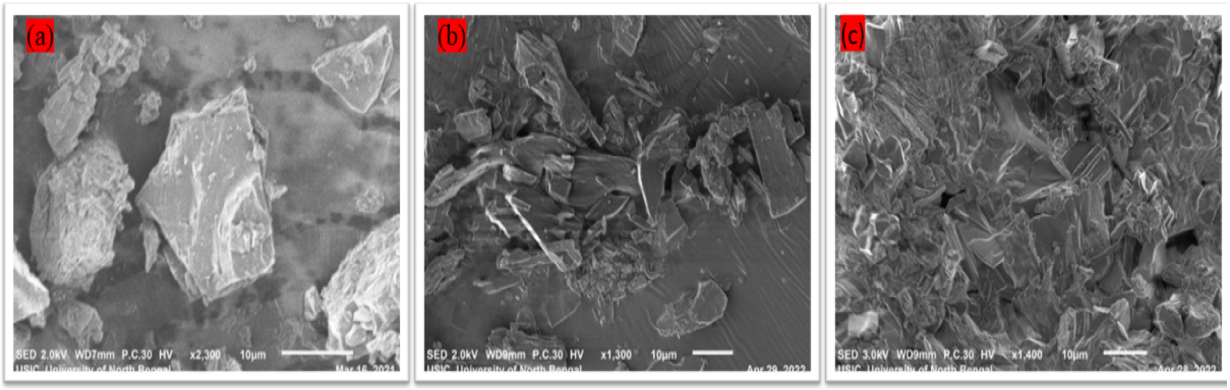

Figure 4. SEM images of (a) β-CD, (b) dyphylline, and (c) IC.

Scheme 3. Plausible Mode of Insertion of Dyphylline Insight into β-CD

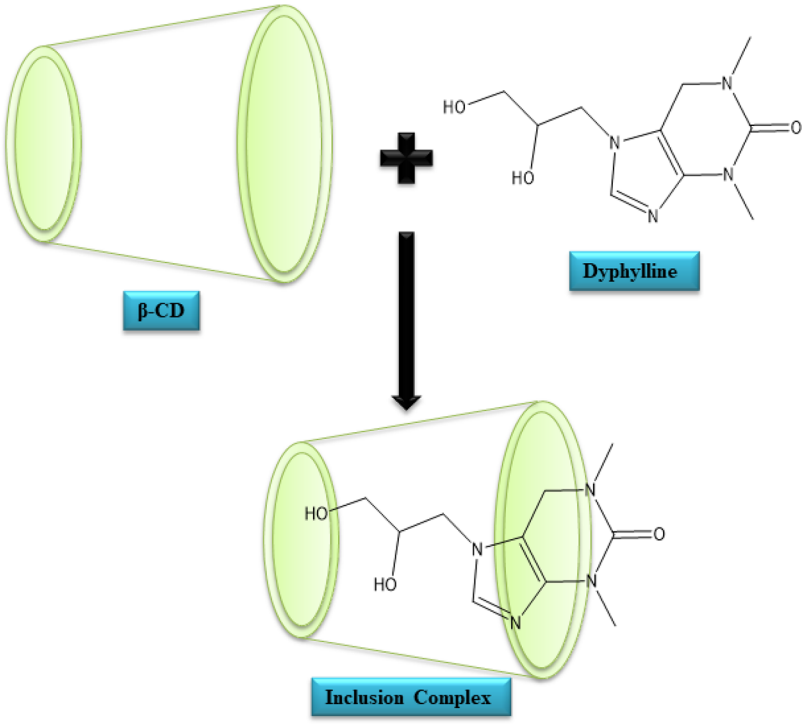

Table 4. Apparent Molar Volume (ϕ_V^0), Viscosity (B), and Viscosity (A) Coefficient and Molar Refraction (R_M^0) of the β-CD + Dyphylline + H_2O System in Aqueous β-CD Solutions of Mass Fractions W_1 = 0.001, 003, and 0.005 at Temperatures 298.15, 303.15, and 308.15 K

temperature T (K)[b]	$\phi_V^0 \times 10^6$ (m^3 mol^{-1})	$S_V^0 \times 10^6$ (m^3 mol$^{-3/2}$ kg$^{1/2}$)	B (dm^3 mol^{-1})	A (dm$^{3/2}$ mol$^{-1/2}$)	R_M^0 (m^3 mol^{-1})
(β-CD + 0.001 dyphylline + H_2O) system					
298.15	178.20	−6.1279	0.4036	0.0486	52.313
303.15	179.51	−7.7966	0.4651	0.0446	52.422
308.15	180.95	−11.8980	0.5457	0.0403	52.553
(β-CD + 0.003 dyphylline + H_2O) system					
298.15	183.82	−13.0490	0.4469	0.0464	52.330
303.15	185.52	−17.9310	0.4948	0.0421	52.454
308.15	188.10	−29.1750	0.5895	0.0357	52.576
(β-CD + 0.005 dyphylline + H_2O) system					
298.15	189.70	−22.9850	0.5025	0.0413	52.384
303.15	192.92	−34.2720	0.5313	0.0392	52.479
308.15	195.77	−41.0290	0.6542	0.0286	52.592

[a]Mass fractions of CDP in the aqueous solution; standard uncertainty in molality u (m) = ±0.0001 mol kg^{-1}. [b]Standard uncertainty in temperature u (T) = ± 0.01 K. Standard uncertainty in pressure u (p) = ±0.01 MPa.

https://doi.org/10.1021/acsomega.2c01902
ACS Omega 2022, 7, 26211−26225

is directly proportional to the temperature and mass fraction of the aqueous β-CD solution, varies linearly with $\sqrt{m}$, and could be least squares fitted to the Masson equation,[36] from which ϕ_V^0 was obtained. The values are presented in Table 4.

$$\phi_V = \phi_V^0 + S_V^* \sqrt{m} \quad (5)$$

The apparent molar volume at infinite dilution and the experimental slope obtained are denoted by ϕ_V^0 and S_V^*, respectively. At infinite dilution, only solvent molecules are present in the vicinity of each solute molecule; hence, ϕ_V^0 is unaffected by solute−solute interaction and is only a measure of solute−solvent interaction.

The ϕ_V^0 values of the examined solute are large and positive in the aqueous β-CD solution at all temperatures studied (Table 4 and Figure S5), indicating the presence of substantial solute−solvent interaction. When ϕ_V^0 and S_V^* values are compared for all solutions and temperatures investigated, ϕ_V^0 is bigger than S_V^*, showing that solute−solvent interactions are more important than solute−solute interactions. Because of the negative values of S_V^* and their decreasing trends with temperature, the solute−solute interaction is absent in the analyzed situations.

Considering the Co-sphere overlap representation,[37,38] there are three dissimilar types of interactions that are possible between dyphylline and β-CD, as follows: (i) hydrophilic−hydrophilic interactions present between hydrophilic groups of dyphylline (such as −OH, C═O, the ring's nitrogen) and hydroxyl groups of β-CD; (ii) hydrophilic−hydrophobic interactions possible between hydrophilic parts of dyphylline and hydrophobic parts of β-CD (hydrophobic cavity); and (iii) hydrophobic−hydrophobic interactions between the hydrophobic groups (alkyl groups) of dyphylline and the hydrophobic portion of β-CD.

The variation of ϕ_V^0 with temperature is suited to a polynomial of the following:

$$\phi_V^0 = a_0 + a_1 T + a_2 T^2 \quad (6)$$

where T is the temperature expressed in K and a_0, a_1, and a_2 are the empirical coefficients depending on the solute, mass fraction of co-solute β-CD. Values of so-obtained coefficients of the above equation for dyphylline in aqueous β-CD are described in Table 5.

Table 5. Values of Various Coefficients of Eq 6 for Dyphylline in Three Different Mass Fractions (w_1) of Aqueous β-CD Mixtures at Three Different Temperatures[a]

aq. IL mixture (w_1)	$a_0 \times 10^6$ (m^3 mol^{-1})	$a_1 \times 10^6$ (m^3 mol^{-1} K^{-1})	$a_2 \times 10^6$ (m^3 mol^{-1} K^{-2})
0.001	335.080	−1.3014	0.0026
0.003	1673.20	−10.243	0.0176
0.005	−671.20	5.0936	−0.0074

[a]Standard uncertainties u (T) = ±0.01 K.

The limiting apparent molar expansibilities, ϕ_E^0, can be evaluated with the help of the following equation:

$$\phi_E^0 = (\delta\phi_V^0/\delta T)_P = a_1 + 2a_2 T \quad (7)$$

The limiting apparent molar expansibilities, ϕ_E^0, vary in magnitude with the changing temperature. Moreover, most importantly, whether the solute is in a long-range structure-making or breaking capacity in the aqueous mixed system can be evaluated by inspecting the sign of $(\delta\phi_E^0/\delta T)_P$ proposed by Hepler.[39]

$$(\delta\phi_E^0/\delta T)_P = (\delta^2\phi_V^0/\delta T^2)_P = 2a_2 \quad (8)$$

A negative sign or small positive value of $(\delta\phi_E^0/\delta T)_P$ indicates that the molecule is a structure-breaker; else, it is a structure-maker.[34,40,41] Table 6 displays that $(\delta\phi_E^0/\delta T)_P$ data

Table 6. Limiting Apparent Molar Expansibility (ϕ_E^0) for Dyphylline in Three Different Mass Fractions (w_1) of Aqueous β-CD Mixtures at Three Different Temperatures[a]

$(\delta\phi_E^0/\delta T)_P \times 10^6$ (m^3 mol^{-1} K^{-2})		
(w_1) 0.001	(w_1) 0.003	(w_1) 0.005
0.0052	0.0352	−0.0148

[a]Standard uncertainty values of u are u (T) = ±0.01 K.

of dyphylline are small positive or negative signs under investigation. The results suggest that solutes are definitely structure-breakers in all of the solutions under observation; i.e., they disrupt the solvent structure by increasing the solute−solvent interactions.

3.9. Viscosity. The viscosity data are measured for the studied systems and reported in Tables S6−S9. The relative viscosity (η_r) has been calculated with the help of the Jones−Dole equation.[42]

$$(\eta/\eta_0 - 1)/\sqrt{m} = (\eta_r - 1)/\sqrt{m} = A + B\sqrt{m} \quad (9)$$

where η_r (η/η_0), η, and η_0 represent the relative viscosity and viscosity of the ternary solution (dyphylline in aqueous β-CD) and solvent (aqueous β-CD), respectively, and m defines the molality of dyphylline in aqueous β-CD. The term A (in eq 9) is called the Falkenhagen coefficient.[43] It is attained with the assistance of the ionic attraction concept of Falkenhagen−Vernon and is specific to the solute−solute interaction, and B is the empirical constant or viscosity B-coefficient, which signifies the solute−solvent interaction that arises in the mixed medium. The values of A- and B-coefficients are calculated by plotting $(\eta_r - 1)/\sqrt{m}$ against $\sqrt{m}$ with the least square technique. The results of reduction of values of A with the rise in temperature of the studied system (dyphylline in aqueous β-CD) are recorded in Table 4 along with data of B-values to be discussed in the next paragraph. The above trend of A-values signifies that the very weak solute−solute (dyphylline−dyphylline) interaction is present over there, and it is also in good agreement with that obtained from S_V^* values.

On the other hand, the viscosity B-coefficient[44] has provided valuable information about the solvation of solutes and their impact on the structure of the solvent in the local vicinity of the solute molecules in solutions. The B-coefficient values are positive as shown in Table 4 and Figure S6, much higher than the A-coefficient, suggesting that the solute−solvent interaction is more favored than the solute−solute interaction. The rising trend of viscosity B-coefficient with temperature and also with the mass fraction of the aqueous β-CD mixture indicates that the developing interaction between the solute and solvent is boosted with increasing temperature as well as the mass fraction of aqueous β-CD solutions.[34,41] These findings are reliable with those obtained using ϕ_V^0 values.

All in all, positive B-coefficients propose kosmotropes because strongly and firmly solvated solutes show a greater change in viscosity, whereas negative B-coefficients specify

https://doi.org/10.1021/acsomega.2c01902
ACS Omega 2022, 7, 26211−26225

Table 7. Values of $(\bar{V}_1^0 - \bar{V}_2^0)$, $\Delta\mu_1^{0\neq}$, $\Delta\mu_2^{0\neq}$, $T\Delta S_2^{0\neq}$, and $\Delta H_2^{0\neq}$ for Dyphylline in Three Different Mass Fractions (w_1) of Aqueous β-CD Mixtures at Three Different Temperatures[a]

parameters	w_1 = 0.001			w_1 = 0.003			w_1 = 0.005		
	T[a] = 298.15 K	303.15 K	308.15 K	T[a] = 298.15 K	303.15 K	308.15 K	T[a] = 298.15 K	303.15 K	308.15 K
				dyphylline					
$(\bar{V}_1^0 - \bar{V}_2^0)\cdot10^6$/m^3·mol^{-1}	−159.00	−160.28	−161.69	−162.36	−164.03	−166.58	−165.98	−169.17	−171.98
$\Delta\mu_1^{0\neq}$/kJ·mol^{-1}	10.26	10.23	10.16	10.57	10.55	10.48	10.85	10.84	10.77
$\Delta\mu_2^{0\neq}$/kJ·mol^{-1}	82.90	92.22	104.27	80.94	87.82	100.48	80.72	85.18	99.75
$T\Delta S_2^{0\neq}$/kJ·mol^{-1}	−637.09	−647.77	−658.45	−582.41	−592.17	−601.94	−567.47	−576.99	−586.50
$\Delta H_2^{0\neq}$/kJ·mol^{-1}	−554.19	−555.55	−554.19	−501.46	−504.35	−501.46	−486.75	−491.80	−486.75

[a]Standard uncertainties values of u are u (T) = ±0.01 K.

chaotropes for weakly and feebly hydrated solutes with concentration.[45] The sign of dB/dT is more indicative in assessing the structure-making or -breaking ability rather than the sign or quantity of the B-coefficient.[46,47] A negative sign of dB/dT implies structure-making (kosmotropic), whereas a positive sign recommends structure-breaking (chaotropic). The theory behind dB/dT is based on Eyring's theory of viscosity,[48] which states that a negative value of dB/dT corresponds to the energy of activation for viscous flow being higher in the case of the solution than in the case of the pure solvent.

The increasing trends of the B-coefficient values with the temperature of the studied solute, dyphylline (positive dB/dT), indicate that the solute is categorized as a structure-breaker.[34,41]

According to Eyring and co-workers,[48,49] the free energy of activation of viscous flow per mole of solvent, $\Delta\mu_1^{0\neq}$, could be evaluated by using the following equation:

$$\eta_0 = (hN_A/\bar{V}_1^0)\exp(\Delta\mu_1^{0\neq}/RT), \quad (10)$$

where h is known as Planck's constant, N_A refers to Avogadro's number, and $\bar{V}_1^0$ is the partial molar volume of the solvent. Equation 10 can be reorganized as follows:

$$\Delta\mu_1^{0\neq} = RT\ln(\eta_0\,\bar{V}_1^0/hN_A). \quad (11)$$

Feakins et al.[50,51] proposed that if eqs 9 and 11 are followed, then

$$B = (\bar{V}_1^0 - \bar{V}_2^0) + \bar{V}_1^0\,[(\Delta\mu_1^{0\neq} - \Delta\mu_2^{0\neq})/RT], \quad (12)$$

where $\bar{V}_2^0$ and $\Delta\mu_2^{0\neq}$ are the limiting partial molar volume (ϕ_V^0) of the solute and ionic activation energy per mole of the solute at infinite dilution. After rearranging eq 12, we have

$$\Delta\mu_2^{0\neq} = \Delta\mu_1^{0\neq} + (RT/\bar{V}_1^0)[B - (\bar{V}_1^0 - \bar{V}_2^0)]. \quad (13)$$

Table 7 indicates that the $\Delta\mu_2^{0\neq}$ values are all positive and much greater than $\Delta\mu_1^0$, implying that the interaction between the solute (dyphylline) and the solvent (aqueous β-CD solution) molecules is less favored in the transition state than in the ground state. The solvation of the solute in the transition state is unfavorable in terms of free energy.

The entropy of activation $(\Delta S_2^{0\neq})$[52] for the solution has been calculated using the following relation:

$$\Delta S_2^{0\neq} = -d(\Delta\mu_2^{0\neq})/dT \quad (14)$$

where $\Delta S_2^{0\neq}$ has been obtained from the negative slope of the plots of $\Delta\mu_2^{0\neq}$ against T by utilizing a least squares method.

The enthalpy of activation $(\Delta H_2^{0\neq})$[52] has been obtained from the following relation:

$$\Delta H_2^{0\neq} = \Delta\mu_2^{0\neq} + T\Delta S_2^{0\neq} \quad (15)$$

The values of $\Delta S_2^{0\neq}$ and $\Delta H_2^{0\neq}$ are also listed and stated in Table 7.

From Table 7, it is clear that for all the mass fractions of the aqueous β-CD solution, the value of $\Delta\mu_1^{0\neq}$ is practically constant, suggesting the dependence of $\Delta\mu_2^{0\neq}$ predominantly only on the viscosity coefficients and $(\bar{V}_1^0 - \bar{V}_2^0)$ terms. Positive $\Delta\mu_2^{0\neq}$ values at all temperatures and solvent compositions studied indicate the complicated and difficult nature of the process of viscous flow as the temperature and mass fraction of the aqueous β-CD solution rise. As a result, the establishment of a transition state is becoming less appealing. Feakins et al.[50−52] recommended that for a substance having $\Delta\mu_2^{0\neq} > \Delta\mu_1^{0\neq}$ and positive B-coefficients, indicating stronger solute−solvent interactions, accordingly implying that the formation of the transition state is followed by rupturing and distorting the intermolecular forces in the solvent structure in the medium.[53] Both the values of $\Delta S_2^{0\neq}$ and $\Delta H_2^{0\neq}$ are negative, indicating that the formation of the transition state is related to bond-making and growing in order. The problem is rendered difficult by the lack of definite proof for the precise mechanism, though it may be recommended that the slip-plane is in the disordered state.[54] According to the Feakins et al. model, as $\Delta\mu_2^{0\neq} > \Delta\mu_1^{0\neq}$, the solute behaves as structure breakers. This approves the dB/dT behavior of the solute in an aqueous β-CD solution.

3.10. Refractive Index. The refractive index (n_D) calculation is also an important tool to investigate the molecular interactions that occur in the solution.[34,55] The molar refraction (R_M) is calculated with the help of the Lorentz−Lorenz relation.[56]

$$R_M = \{(n_D^2 - 1)/(n_D^2 + 2)\}(M/\rho) \quad (16)$$

where R_M stands for molar refraction, n_D for refractive index, M for molar mass, and ρ for density of the solution, respectively. The ratio c_o/c is the refractive index of a material, where c describes the velocity of light in the medium and c_o is the velocity of light in a vacuum. Expressed more essentially that the refractive index of a compound represents its capacity to refract light as it passes starting with one medium and then onto the next, and in this manner, the higher a compound's refractive index is, the more the light is refracted.[57] According to Deetlefs et al.,[58] a substance's refractive index is higher when its molecules are more closely packed or when the compound is denser in general. As a result, a review of Tables S6 and S9 revealed the high values of refractive index and molar refraction for the studied solute dyphylline in all mass fractions of the aqueous β-CD solution, implying that the molecules are more tightly packed in the ternary mixture.

https://doi.org/10.1021/acsomega.2c01902
ACS Omega 2022, 7, 26211−26225

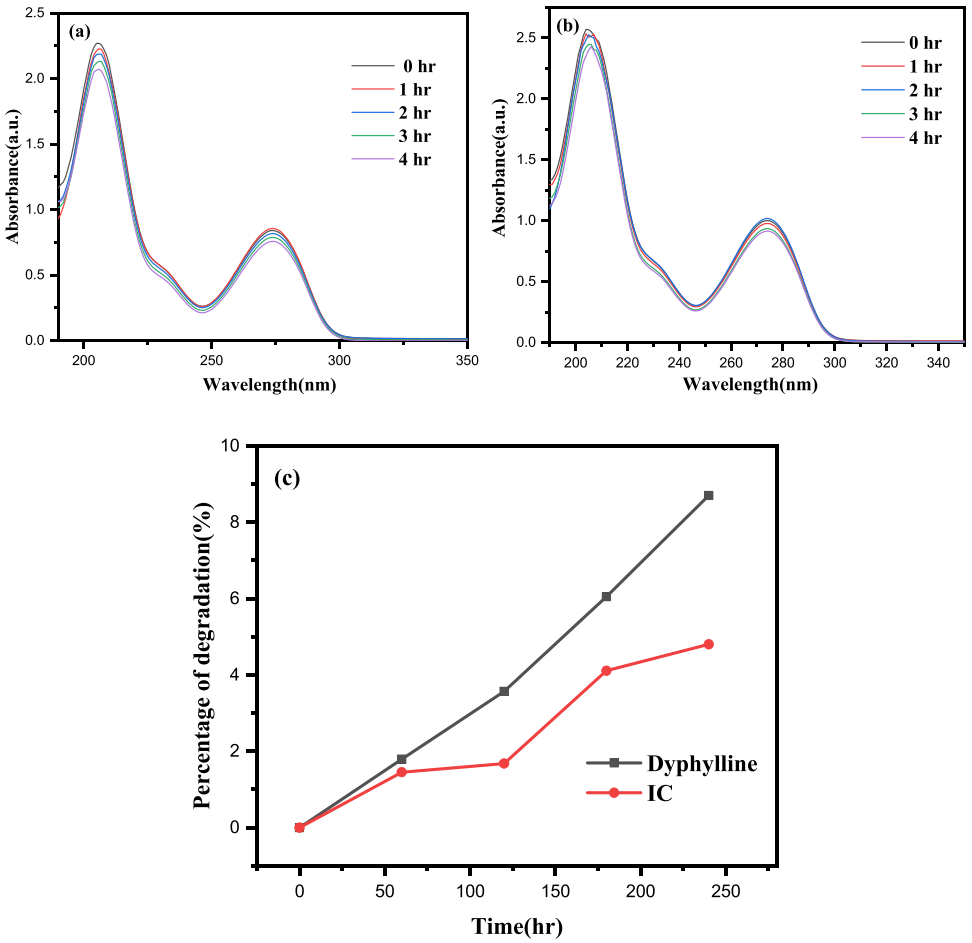

Figure 5. Time-dependent UV−vis spectra of (a) dyphylline and (b) IC and (c) percentage of degradation of each component under sunlight.

The limiting molar refraction (R_M^0) was calculated from the following eq 17 and listed in Table 2:

$$R_M = R_M^0 + R_S\sqrt{m} \quad (17)$$

Accordingly, we found that (Table 4 and Figure S7) the values of R_M^0 increase as the temperature rises, as does the mass fraction of the aqueous β-CD solution, implying that the solute−solvent relationship is reinforced as the temperature and mass fraction of the aqueous β-CD solution rise. The large values of R_M^0 values of dyphylline in the aqueous β-CD solution in all respects indicate that a strong solute−solvent interaction prevails in the ternary solution. These findings are consistent with those obtained from the apparent molar volume ϕ_V^0 and viscosity B-coefficient values discussed previously.

3.11. Photostability Test. The photodecomposition of both the free medicine dyphylline and the IC, when exposed to sunlight, was examined. We conducted photodegradation tests to compare the photostability of IC to that of pure dyphylline, comparing the UV spectra of both the guest and IC complex before and after exposure to sunlight, and we discovered a shift in spectral intensity.[59] We made a 100 mM 40 mL solution of both the dyphylline and the IC and placed them in two separate 100 mL beakers. After that, these two reaction mixtures were magnetically stirred for 45 min to produce adsorption−desorption equilibrium. The reaction mixtures' photodecomposition performance was then examined by exposing them to visible sunlight. Following the photostability experiment, a fixed amount (in mL) of aliquots of each solution was extracted at a predetermined time interval in a UV−vis spectrophotometer to determine their concentration in terms of absorbance change at 206 nm (Figure 5a,b). The following equation was used to compute the percentage of degradation:

$$\%\ \text{of degradation} = (A_0 - A_t) \times 100/A_0 \quad (18)$$

A_0 represents the dyphylline (or IC) solution's starting absorbance, and A_t represents the solution's ultimate absorbance after time t for each procedure (in hours). When these two values are compared, it can be shown that when exposed to sunlight, pure dyphylline degrades more than IC. In 4 h, the degradation percentage for pure dyphylline was 8.70%, while the degradation rate for IC was just 4.80% (Figure 5c). This indicates that the photostability of formed IC is higher than that of pure dyphylline, proving the utility of β-CD complexation in boosting dyphylline photostability.[60]

3.12. CT-DNA Binding Study: The Procedure for Discharging a Guest from the Cavity of β-CD. Many drugs are already in use or in advanced clinical trials to target DNA to treat or control the condition.[24,61] These drugs obstruct or modify DNA function to treat disorders like asthma, emphysema, cardiac dyspnea, cancer, etc. It is unclear how pharmaceutical molecules interact with DNA, according to scientists. As a result, DNA interaction research is fascinating and important not just for understanding drug−DNA interaction mechanisms but also for developing new and

https://doi.org/10.1021/acsomega.2c01902
ACS Omega 2022, 7, 26211−26225

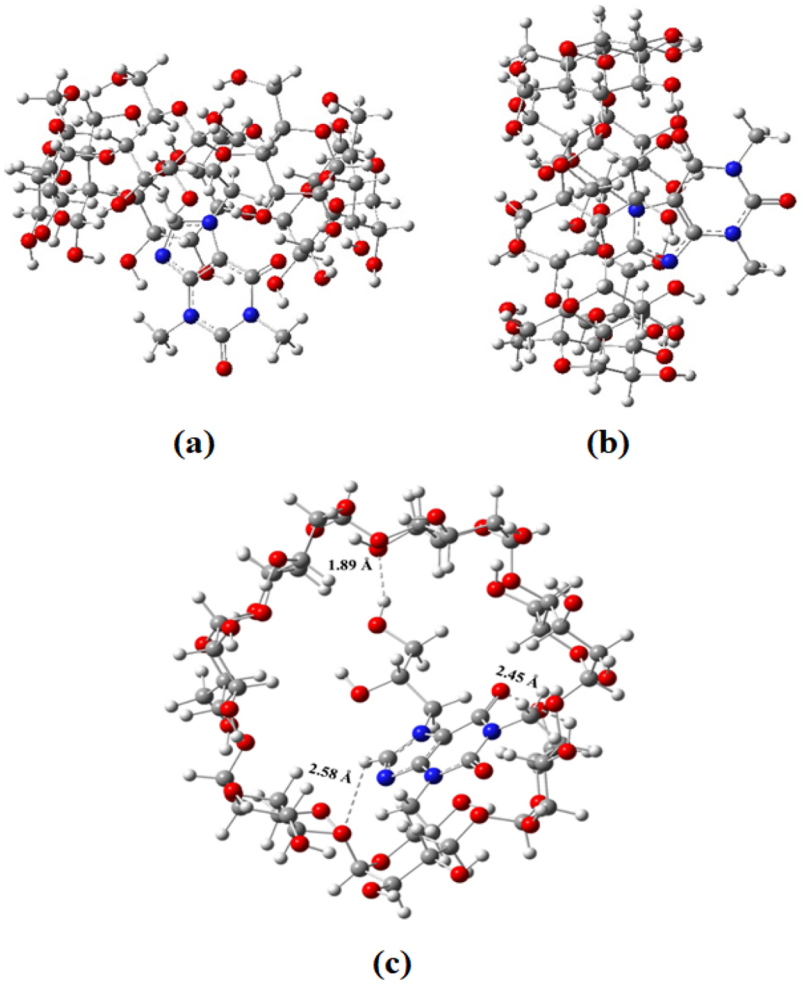

Figure 6. (a) Optimized geometries for the dyphylline−β-CD complex at the M06-2X/6-31+G (d) level of theory. (b) Side views and (c) top view.

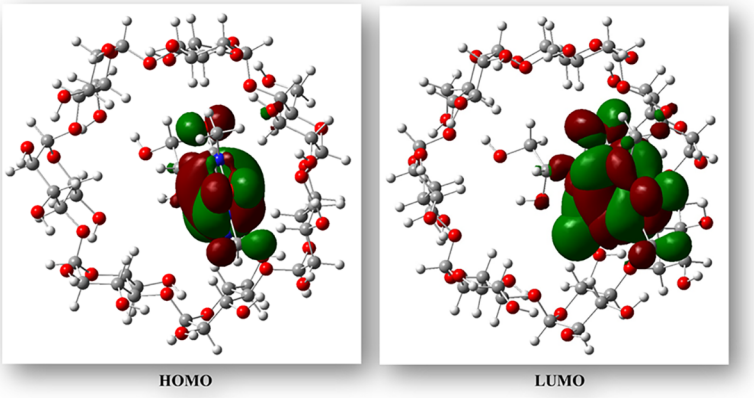

Figure 7. HOMO and LUMO charge densities of dyphylline−β-CD complex.

more effective DNA-targeted treatments. Our main goal is to see how our synthesized IC interacts with DNA and how β-CD influences drug−DNA interactions, which could help us design new drugs or improve the efficacy of existing ones. With a 30 min incubation period after each addition of CT-DNA, the UV spectra of a fixed concentration (25 μM) of drug and IC were taken with varied CT-DNA concentrations (Figure S8). Using the following relation, the spectral data were utilized to create a Benesi−Hildebrand plot:[62]

$$\frac{1}{\Delta A} = \frac{1}{\Delta A[\text{dyphylline}]K\text{BH}^*}\frac{1}{[M]} + \frac{1}{\Delta A[\text{dyphylline}]} \quad (19)$$

where $[M]$ is the concentration of DNA, $[\Delta A]$ is the change in absorbance at a certain wavelength, and $\Delta A[\text{dyphylline}]$ is the maximum absorbance. The Benesi−Hildebrand association constant (K_{BH}) for complex formation was determined from the ratio of the intercept to the slope by graphing the

https://doi.org/10.1021/acsomega.2c01902
ACS Omega 2022, 7, 26211−26225

Table 8. Zone of Inhibition of Tested Samples against Different Bacteria Studied (Data Presented as Mean ± SD of Triplicate Determination)

tested microorganism	sample name	zone of inhibition (in millimeter)		
		5 mM	10 mM	20 mM
S. aureus	β-CD	0	0	0
	dyphylline	0	0	14.667 ± 0.577
	IC	15.33 ± 0.577	15 ± 1	19
B. megaterium	β-CD	0	0	15.667 ± 2.517
	dyphylline	0	14.333 ± 0.577	15.333 ± 0.577
	IC	15.33 ± 0.577	17 ± 1	19.667 ± 0.577
B. subtilis	β-CD	0	0	10.333 ± 0.577
	dyphylline	0	0	20 ± 1
	IC	0	11.667 ± 1.528	16.667 ± 1.155
E. coli	β-CD	0	6.667 ± 0.577	16.333 ± 0.577
	dyphylline	0	7.667 ± 1.528	15 ± 1
	IC	15 ± 1	20 ± 1	23.333 ± 1.155
S. typhimurium	β-CD	0	0	0
	dyphylline	0	0	14.667 ± 0.577
	IC	15.33 ± 0.57	17.33 ± 0.57	19 ± 1

reciprocal of the difference in absorbance with regard to the reciprocal of the DNA concentration.

Both the drug and the IC showed a hyperchromic shift with a minor bathochromic shift in UV−vis spectra, confirming an intercalating binding mechanism with DNA (Figure S8). The binding constants (K_{BH}/M^{-1}) are listed and found to be 1.70×10^4 and 1.05×10^4 for pure dyphylline and IC, respectively. The drug's DNA binding constant was discovered to be greater than the IC, which could be connected to the creation of IC, which inhibits the drug from intercalating with DNA.[30] As a result of this experiment, we may assume that, in the presence of CT-DNA, the seeping of the guest molecule from the hollow of CDs into the aqueous solution is regular.[24,63]

3.13. Theoretical Study of Host−Guest Interaction. Optimized geometries of the dyphylline−β-CD complex are presented in Figure 6. The imidazole ring including the side chain of dyphylline enters into the cavity of β-CD fully, while the rest of the part remains outside the cavity of β-CD. The strong interaction of dyphylline with β-CD has been confirmed by the residual short bonds ranging from 1.89 to 2.58 Å. Hydrogen bonding interactions between the H atom of the −OH group present in the side chain, and N atoms of the imidazole ring of dyphylline with the −OH group of β-CD which accounts for the high adsorption energy (E_{ads} = −5.50 eV) in the aqueous medium (Table S13).

HOMO and LUMO charge densities (Figure 7) were analyzed to understand the host−guest interaction and the amount of charge transfer occurring in this complex system. We found that HOMO and LUMO densities are distributed mostly on the dyphylline, confirming that charge transfer is less prominent involving this complex.

To understand the type of interactions between the dyphylline and β-CD complex, we have analyzed the molecular electrostatic potential maps (ESP), as shown in Figure S9. The red region of ESP maps around the β-CD cavity further signifies the stronger and more prominent interactions that exist involving dyphylline and β-CD.

To visualize the weak interactions operating in dyphylline−β-CD, we have analyzed the reduced density gradient (RDG) plots as shown in Figure S10. Weak interactions like H-bonding, van der Waals interactions, and steric interactions also known as noncovalent interactions have been studied by considering the noncovalent index (NCI) obtained from the plots of RDG vs the product of electron density and the sign of the second Hessian eigenvalue [$\text{sign}(\lambda 2)\rho(r)$] for the inclusion complex. By analyzing the RDG plot, one can simply differentiate between attractive and repulsive interactions operating in inclusion complexes. Negative values of $\text{sign}(\lambda 2)\rho$ indicate attractive interactions, while repulsive interactions are characterized by positive values of the same. We found that very strong H-bonding interactions (attractive interactions) are operating between dyphylline and β-CD units as indicated by the large scattered area of the negative region of the RDG plot (0.02−0.03 region).

3.14. Comparative Antibacterial Activity of Dyphylline, β-CD, and Its Inclusion Complex (IC). The inclusion complex showed potent bactericidal activity against both Gram-positive and Gram-negative bacteria as evident by the zone of inhibition. There was no zone of inhibition observed against all the studied microorganisms at a very low concentration (5 mM) of both host (β-CD) and guest (dyphylline). Dyphylline in a medium dosage (10 mM) displayed bactericidal activity against *B. megaterium* and *E. coli*, and in the same dose, β-CD showed minute efficacy only against Gram-negative *E. coli* (Table 8). Meanwhile, no efficacy of β-CD was observed against Gram-positive *S. aureus* and Gram-negative *S. typhimurium* (Figures S11 and 9). However, *B. subtilis* IC exhibited a bactericidal effect at a very low concentration (5 mM) and showed dose-dependent antimicrobial activity against all of the studied microorganisms as corroborated by the inhibition zone study (Table 8). Among the studied Gram-positive bacteria, *B. megaterium* was the most susceptible to IC, and this particular IC at a high concentration showed more pronounced effects on Gram-negative *E. coli* than *S. typhimurium* (Figures 8 and 9). As stated previously, dyphylline is a theophylline derivative having bronchodilator and vasodilator effects. Past *in vitro* and *in vivo* studies reported the antifungal activity of theophylline against different species of dermatophytes.[64]

However, very limited information is available about the antibacterial effects of theophylline, and with regard to dyphylline, no report of bactericidal effects has been published to date as far as we know. Our investigation confirmed that Gram-negative bacteria were more susceptible to the tested

https://doi.org/10.1021/acsomega.2c01902
ACS Omega 2022, 7, 26211−26225

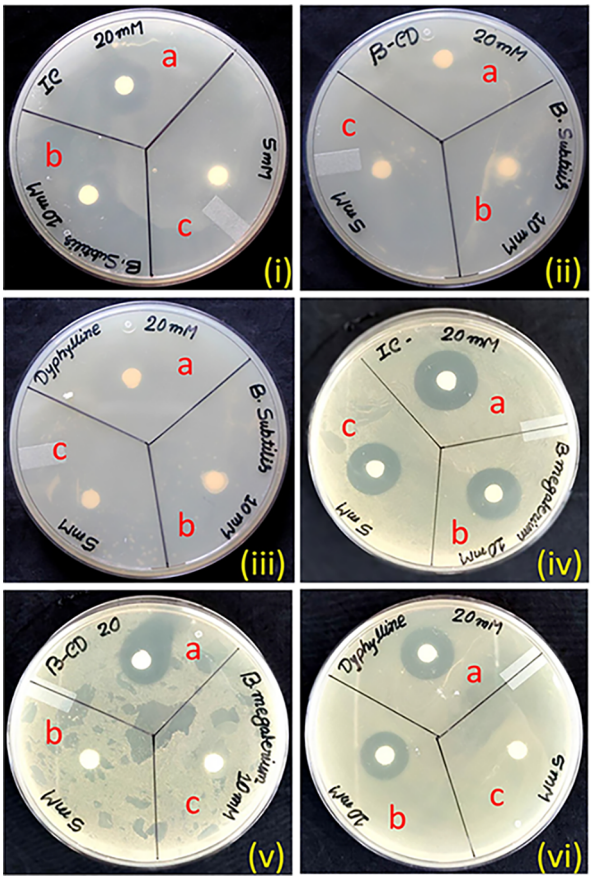

Figure 8. Antimicrobial activity of (i, iv) IC, (iii, v) β-CD, and (iii, vi) dyphylline against (i, ii, iii) *B. subtilis* and (iv, v, vi) *B. megaterium* (concentration of the sample applied: a = 20 mM, b = 10 mM, c = 5 mM).

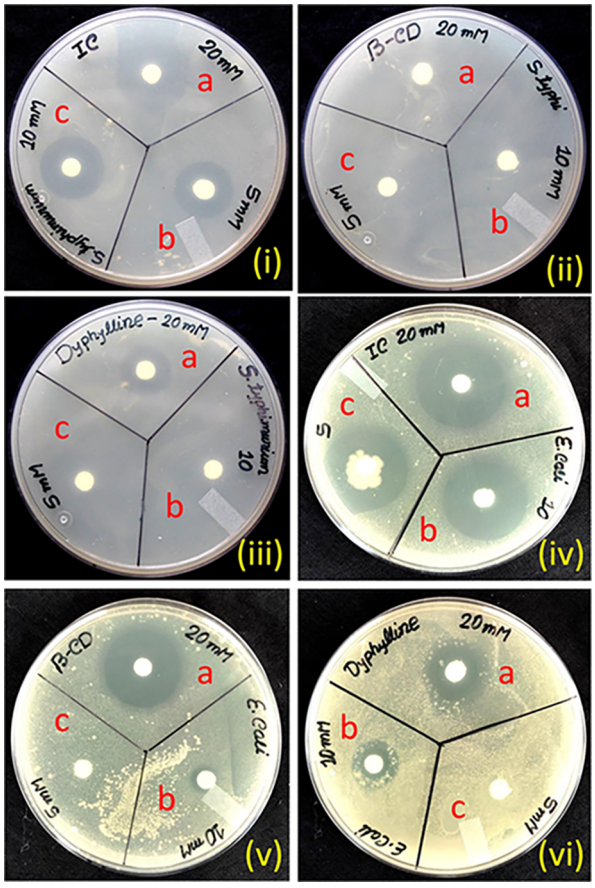

Figure 9. Antimicrobial activity of (i, iv) IC, (iii, v) β-CD, and (iii, vi) dyphylline against (i, ii, iii) *S. typhimurium* and (iv, v, vi) *E. coli* (concentration of the sample applied: a = 20 mM, b = 10 mM, c = 5 mM).

samples than the Gram-positive bacteria, which may be due to the presence of a thick peptidoglycan layer in Gram-positive bacterial cell making them more resistant as this layer protects the entry of desired chemical inside bacterial cell.[17] Borkowski et al.,[65] in an antibacterial study on the application of theophylline-based ionic liquids, demonstrated that this chemical mainly creates cellular damage and deformed the bilayer, which ultimately leads to necrosis. The detailed mechanism of the dyphylline based inclusion complex includes the (a) absorption and penetration of the sample into the cell wall; (b) deactivation of membrane proteins and loss of regulation of metabolic processes; (c) distortion of the lipid bilayer and leakage of intracellular material; (d) formation of phospholipid micelles and further breakdown of the bilayer; and (e) cell lysis.[66] Ruddarraju et al.[67] also reported potent antimicrobial and anticancer activities of theophylline containing acetylenes derivatives.

The bactericidal activity of dyphylline greatly increased on formation of the inclusion complex (IC) with β-CD, which may be due to complexation, Cyclodextrin significantly improves the solubility of drugs, which makes the drugs (dyphylline) highly available at the site of action.[68,69]

3.15. Toxicity Study. After the drug treatment, the viability of the cancer cell line was decreased. The percentage of cytotoxicity resembles the loss of cellular viability during drug treatment.[24,27] The more toxic the drug is, the more it can reduce the reproducibility of a cell. In case of the kidney cancer cell line (ACHN), the cytotoxicity caused by IC is much higher than the toxicity caused by the control drug (dyphylline). In the inclusion-complex-treated cells, there is a significant loss of cells observed when compared with the control-drug-treated cells.[24,27] This observation indicates that the inclusion complex is more toxic than the control one (Figure 10). The IC_{50} value signifies the loss of initial cellular density to its 50% concentration. From the depicted graph, the IC_{50} values for each of the drugs were calculated and provided in a separate table. The differences in 50% inhibitory concentration (IC_{50}) also designate the information that the cells resemble different cellular responses during different drug treatments and therefore the cellular viabilities differ from each other under the same experimental condition. As the IC_{50} dose is less in case of IC (9.87 μM) than dyphylline (10.68 μM), therefore, from the obtained data, it is clear that IC is more capable of inducing toxicity to cancer cells when compared with dyphylline.

This finding states that the inclusion complex is more toxic than the control drug. Therefore, the above experimental data have proven that this inclusion complex can be considered as a potent anticancer drug to treat renal carcinoma.

4. CONCLUSIONS

The most widely used drug dyphylline produces a host−guest IC with β-CD, according to the findings. The inclusion phenomenon is confirmed by the UV−vis Job's plot, surface tension, and conductivity investigations that show that a 1:1 IC

https://doi.org/10.1021/acsomega.2c01902
ACS Omega 2022, 7, 26211−26225

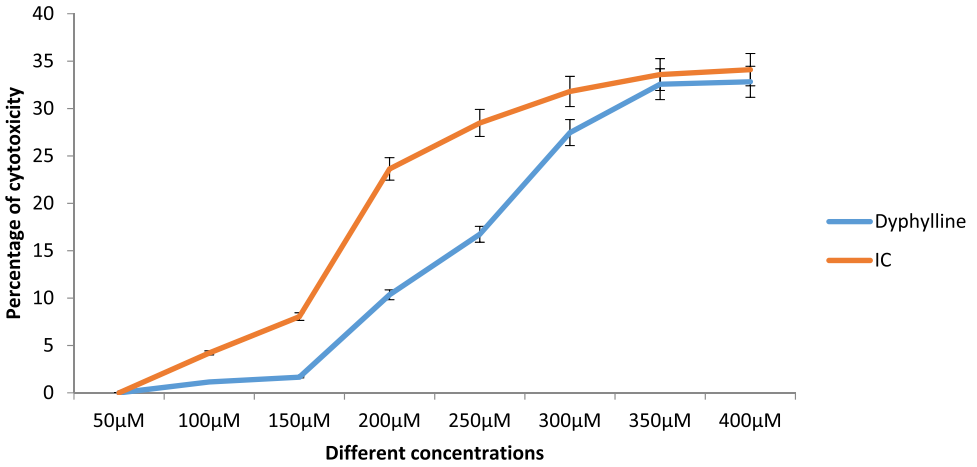

Figure 10. Percentage of cytotoxicity of dyphylline and IC at different concentrations.

has formed. All of the estimated density, viscosity, and refractive index values obtained from the additional data strongly support the establishment of the IC and the solute−solvent interaction observed in the investigated solution systems. The significance of the work is quantitatively explained by the determination of association constants and several thermodynamic characteristics. As shown by ^{1}H NMR spectroscopic analysis, the aromatic component of dyphylline was inserted from the side of the larger rim of the cavity of β-CD. In the presence of CT-DNA, the controlled discharge of dyphylline molecules from the hydrophobic cavity to the polar aqueous media has been effectively documented, which may reduce toxicity inside the body. As a result, there's a significant chance that dyphylline and CT-DNA will connect similarly in the human body, allowing the right amount of dyphylline to be delivered to the right place. Furthermore, dyphylline's antibacterial activity and photostability in the presence of sunlight were greatly improved after being encapsulated in β-CD. The potent bactericidal activity of the inclusion complex as evident from the antibacterial study could be useful in the development of new antibiotics. DFT studies indicate that dyphylline and β-CD form a stable inclusion complex and account for very high adsorption energy (E_{ads} = −5.50 eV), corroborating experimental observations. All of the evidence points to the formation of IC, and the current study examines its suitability for a variety of applications in modern biomedical sciences as a regulated delivery technique.

CREDIT AUTHOR STATEMENTS

Mahendra Nath Roy, Modhusudan Mondal: Conceptualization, Resources. Mahendra Nath Roy: Supervision. Modhusudan Mondal, Subhankar Choudhury & Md Salman Haydar: Writing - review & editing. Modhusudan Mondal, Shatarupa Basak, Md Salman Haydar, Narendra Nath Ghosh: Investigation, Writing - original draft, Methodology, Software, Formal analysis. Modhusudan Mondal, Shatarupa Basak, Biswajit Ghosh, Md Salman Haydar: Validation, Investigation, Visualization.

ASSOCIATED CONTENT

Supporting Information

The Supporting Information is available free of charge at https://pubs.acs.org/doi/10.1021/acsomega.2c01902.

Detailed descriptions of all the chemicals used, conductance data table, surface tension data table, Job's plot table, association constant data, density, viscosity data table, energy calculations of both inclusion complexes using computational studies, ^{1}H NMR figures, and all the related figures associated with data (PDF)

AUTHOR INFORMATION

Corresponding Author

Mahendra Nath Roy − *Department of Chemistry, University of North Bengal, Darjeeling 734013, India; Vice-Chancellor, Alipurduar University, Alipurduar 736122, India;* orcid.org/0000-0002-7380-5526; Email: mahendraroy2002@yahoo.co.in

Authors

Modhusudan Mondal − *Department of Chemistry, University of North Bengal, Darjeeling 734013, India*

Shatarupa Basak − *Department of Chemistry, University of North Bengal, Darjeeling 734013, India*

Debadrita Roy − *Department of Chemistry, University of North Bengal, Darjeeling 734013, India*

Md Salman Haydar − *Nanobiology and Phytotherapy Laboratory, Department of Botany, University of North Bengal, Darjeeling 734013, India*

Subhankar Choudhury − *Department of Chemistry, Malda College, Malda 732101, India*

Biswajit Ghosh − *Department of Chemistry, University of North Bengal, Darjeeling 734013, India*

Narendra Nath Ghosh − *Department of Chemistry, University of Gour Banga, Malda 732103, India*

Ankita Dutta − *Department of Biotechnology, University of North Bengal, Darjeeling 734013, India*

Palash Mandal − *Nanobiology and Phytotherapy Laboratory, Department of Botany, University of North Bengal, Darjeeling 734013, India*

Kanak Roy − *Department of Chemistry, Alipurduar University, Alipurduar 736122, India*

Anoop Kumar − *Department of Biotechnology, University of North Bengal, Darjeeling 734013, India*

Complete contact information is available at: https://pubs.acs.org/10.1021/acsomega.2c01902

https://doi.org/10.1021/acsomega.2c01902
ACS Omega 2022, 7, 26211−26225

Notes

The authors declare no competing financial interest.

■ ACKNOWLEDGMENTS

Prof. M.N. Roy would like to express his gratitude to the University Grants Commission (UGC), New Delhi, Government of India, for providing the study with the necessary resources. M. Mondal and S. Basak are grateful to the UGC for awarding them a Junior Research Fellows scholarship with reference numbers 191620113148 and 272/(CSIR-UGC NET JUNE 2017), respectively. The authors are also thankful to the Nanobiology and Phytotherapy Laboratory, Department of Botany, University of North Bengal, for biological activity experiments.

■ REFERENCES

(1) Villiers, A. Sur la fermentation de la fécule par l'action du ferment butyrique. *Compt. Rend. Acad. Sci.* **1891**, *112*, 536−538.
(2) Dinar, K.; Sahra, K.; Seridi, A.; Kadri, M. Inclusion complexes of N-sulfamoyloxazolidinones with β-cyclodextrin: A molecular modeling approach. *Chem. Phys. Lett.* **2014**, *595*, 113−120.
(3) Szejtli, J. Introduction and general overview of cyclodextrin chemistry. *Chem. Rev.* **1998**, *98*, 1743−1754.
(4) Yang, L.-J.; Ma, S.-X.; Zhou, S.-Y.; Chen, W.; Yuan, M.-W.; Yin, Y.-Q.; Yang, X.-D. Preparation and characterization of inclusion complexes of naringenin with β-cyclodextrin or its derivative. *Carbohydr. Polym.* **2013**, *98*, 861−869.
(5) Mathapa, B. G.; Paunov, V. N. Cyclodextrin stabilised emulsions and cyclodextrinosomes. *Phys. Chem. Chem. Phys.* **2013**, *15*, 17903−17914.
(6) Del Valle, E. M. Cyclodextrins and their uses: a review. *Process Biochem.* **2004**, *39*, 1033−1046.
(7) Gao, Y.; Zhao, X.; Dong, B.; Zheng, L.; Li, N.; Zhang, S. Inclusion complexes of β-cyclodextrin with ionic liquid surfactants. *J. Phys. Chem. B* **2006**, *110*, 8576−8581.
(8) Ma, Y. J.; Jiang, D. Q.; Meng, J. X.; Li, M. X.; Zhao, H. H.; Wang, Y.; Wang, L. Q. Theophylline: a review of population pharmacokinetic analyses. *J. Clin. Pharm. Ther.* **2016**, *41*, 594−601.
(9) Fernandes, J. A.; Sardo, M.; Mafra, L.; Choquesillo-Lazarte, D.; Masciocchi, N. Design, X-ray and NMR crystallography studies of novel theophylline cocrystals prepared by liquid assisted grinding. *Cryst. Growth Des.* **2015**, *15*, 3674−3683.
(10) Chang, S.-Y.; Sun, C. C. Superior plasticity and tabletability of theophylline monohydrate. *Mol. Pharmaceutics* **2017**, *14*, 2047−2055.
(11) Shannon, M. Predictors of major toxicity after theophylline overdose. *Ann. Intern. Med.* **1993**, *119*, 1161−1167.
(12) Caso, J. V.; Russo, L.; Palmieri, M.; Malgieri, G.; Galdiero, S.; Falanga, A.; Isernia, C.; Iacovino, R. Investigating the inclusion properties of aromatic amino acids complexing beta-cyclodextrins in model peptides. *Amino Acids* **2015**, *47*, 2215−2227.
(13) Frisch, M.; Trucks, G.; Schlegel, H.; Scuseria, G.; Robb, M.; Cheeseman, J.; Scalmani, G.; Barone, V.; Petersson, G.; Nakatsuji, H. *Gaussian 16*; revision a. 03. 2016; Gaussian Inc., 2016, *2* (4).
(14) Ghosh, T.; Mondal, S.; Maiti, R.; Nawaz, S. M.; Ghosh, N. N.; Dinda, E.; Biswas, A.; Maity, S. K.; Mallik, A.; Maiti, D. K. Complementary amide-based donor−acceptor with unique nano-scale aggregation, fluorescence, and band gap-lowering properties: a WORM memory device. *Nanotechnology* **2020**, *32*, No. 025208.
(15) Cossi, M.; Barone, V.; Cammi, R.; Tomasi, J. Ab initio study of solvated molecules: a new implementation of the polarizable continuum model. *Chem. Phys. Lett.* **1996**, *255*, 327−335.
(16) Lu, T.; Chen, F. Multiwfn: a multifunctional wavefunction analyzer. *J. Comput. Chem.* **2012**, *33*, 580−592.
(17) Haydar, M. S.; Das, D.; Ghosh, S.; Mandal, P. Implementation of mature tea leaves extract in bioinspired synthesis of iron oxide nanoparticles: preparation, process optimization, characterization, and assessment of therapeutic potential. *Chem. Pap.* **2022**, *76*, 491−514.
(18) Saha, S.; Ray, T.; Basak, S.; Roy, M. N. NMR, surface tension and conductivity studies to determine the inclusion mechanism: thermodynamics of host−guest inclusion complexes of natural amino acids in aqueous cyclodextrins. *New J. Chem.* **2016**, *40*, 651−661.
(19) Rajbanshi, B.; Saha, S.; Das, K.; Barman, B. K.; Sengupta, S.; Bhattacharjee, A.; Roy, M. N. Study to probe subsistence of host-guest inclusion complexes of α and β-cyclodextrins with biologically potent drugs for safety regulatory dischargement. *Sci. Rep.* **2018**, *8*, 1−20.
(20) Saha, S.; Roy, A.; Roy, K.; Roy, M. N. Study to explore the mechanism to form inclusion complexes of β-cyclodextrin with vitamin molecules. *Sci. Rep.* **2016**, *6*, 1−12.
(21) Piñeiro, Á.; Banquy, X.; Pérez-Casas, S.; Tovar, E.; García, A.; Villa, A.; Amigo, A.; Mark, A. E.; Costas, M. On the characterization of host− guest complexes: surface tension, calorimetry, and molecular dynamics of cyclodextrins with a non-ionic surfactant. *J. Phys. Chem. B* **2007**, *111*, 4383−4392.
(22) Gao, Y. A.; Li, Z. H.; Du, J. M.; Han, B. X.; Li, G. Z.; Hou, W. G.; Shen, D.; Zheng, L. Q.; Zhang, G. Y. Preparation and characterization of inclusion complexes of β-cyclodextrin with ionic liquid. *Chem* **2005**, *11*, 5875−5880.
(23) Roy, M. N.; Saha, S.; Barman, S.; Ekka, D. Host−guest inclusion complexes of RNA nucleosides inside aqueous cyclodextrins explored by physicochemical and spectroscopic methods. *RSC Adv.* **2016**, *6*, 8881−8891.
(24) Mondal, M.; Basak, S.; Roy, D.; Saha, S.; Ghosh, B.; Ali, S.; Ghosh, N. N.; Dutta, A.; Kumar, A.; Roy, M. N. Cyclic oligosaccharides as controlled release complexes with food additives (TZ) for reducing hazardous effects. *J. Mol. Liq.* **2022**, *348*, No. 118429.
(25) Job, P. Formation and stability of inorganic complexes in solution. *Ann. Chim.: Sci.* **1928**, *9*, 113−134.
(26) Renny, J. S.; Tomasevich, L. L.; Tallmadge, E. H.; Collum, D. B. Method of continuous variations: applications of job plots to the study of molecular associations in organometallic chemistry. *Angew. Chem., Int. Ed.* **2013**, *52*, 11998−12013.
(27) Bomzan, P.; Roy, N.; Rai, V.; Roy, D.; Ghosh, S.; Kumar, A.; Roy, K.; Chakrabarty, R.; Das, J.; Dakua, V. K.; Basnet, K.; Roy, M. N. Inclusion of an Antiplatelet Agent inside into β-Cyclodextrin for Biochemical Applications with Diverse Authentications: Highlights. *Food Chem. Adv.* **2022**, No. 100015.
(28) Cramer, F.; Saenger, W.; Spatz, H.-C. Inclusion compounds. XIX. 1a The formation of inclusion compounds of α-cyclodextrin in aqueous solutions. Thermodynamics and kinetics. *J. Am. Chem. Soc.* **1967**, *89*, 14−20.
(29) He, Y.; Shen, X. Interaction between β-cyclodextrin and ionic liquids in aqueous solutions investigated by a competitive method using a substituted 3H-indole probe. *J. Photochem. Photobiol. A.* **2008**, *197*, 253−259.
(30) Ghosh, B.; Roy, N.; Roy, D.; Mandal, S.; Ali, S.; Bomzan, P.; Roy, K.; Roy, M. N. An extensive investigation on supramolecular assembly of a drug (MEP) with βCD for innovative applications. *J. Mol. Liq.* **2021**, *344*, No. 117977.
(31) Wang, T.; Wang, M. D.; Ding, C. D.; Fu, J. J. Monobenzimidazole functionalized β-cyclodextrins as supramolecular nanovalves for pH-triggered release of p-coumaric acid. *Chem. Commun.* **2014**, *50*, 12469−12472.
(32) Sierpe, R.; Noyong, M.; Simon, U.; Aguayo, D.; Huerta, J.; Kogan, M. J.; Yutronic, N. Construction of 6-thioguanine and 6-mercaptopurine carriers based on βcyclodextrins and gold nanoparticles. *Carbohydr. Polym.* **2017**, *177*, 22−31.
(33) Schneiderman, E.; Stalcup, A. M. Cyclodextrins: a versatile tool in separation science. *J. Chromatogr. B. Biomed. Sci. Appl.* **2000**, *745*, 83−102.
(34) Mondal, M.; Basak, S.; Choudhury, S.; Ghosh, N. N.; Roy, M. N. Investigation of molecular interactions insight into some biologically active amino acids and aqueous solutions of an antimalarial drug by physicochemical and theoretical approach. *J. Mol. Liq.* **2021**, *341*, No. 116933.

https://doi.org/10.1021/acsomega.2c01902
ACS Omega 2022, 7, 26211−26225

(35) Ekka, D.; Roy, M. N. Molecular interactions of α-amino acids insight into aqueous β-cyclodextrin systems. *Amino Acids* **2013**, *45*, 755−777.
(36) Masson, D. O. XXVIII. Solute molecular volumes in relation to solvation and ionization. *London, Edinburgh Dublin Philos. Mag. J. Sci.* **1929**, *8*, 218−235.
(37) Pal, A.; Kumar, B. Volumetric and acoustic properties of binary mixtures of the ionic liquid 1-butyl-3-methylimidazolium tetrafluoroborate [bmim][BF4] with alkoxyalkanols at different temperatures. *J. Chem. Eng. Data* **2012**, *57*, 688−695.
(38) Zafarani-Moattar, M. T.; Asadzadeh, B.; Shahrisa, A.; Nazari, M. G. Study of thermodynamic properties of l-serine in aqueous 1-carboxymethyl-3-methylimidazolium chloride solutions at 298.15 K. *Fluid Phase Equilib.* **2014**, *363*, 32−40.
(39) Hepler, L. G. Thermal expansion and structure in water and aqueous solutions. *Can. J. Chem.* **1969**, *47*, 4613−4617.
(40) Roy, M. N.; Dakua, V. K.; Sinha, B. Partial molar volumes, viscosity B-coefficients, and adiabatic compressibilities of sodium molybdate in aqueous 1, 3-dioxolane mixtures from 303. 15 to 323.15 K. *Int. J. Thermophys.* **2007**, *28*, 1275−1284.
(41) Mondal, M.; Basak, S.; Rajbanshi, B.; Choudhury, S.; Ghosh, N. N.; Roy, M. N. Subsistence of Diverse Interactions of Some Biologically Important Molecules in Aqueous Ionic Liquid Solutions at Various Temperatures by Experimental and Theoretical Investigation. *J. Mol. Struct.* **2022**, No. 132571.
(42) Jones, G.; Dole, M. The Viscosity of Aqueous Solutions of Strong Electrolytes with Special Reference to Barium Chloride. *J. Am. Chem. Soc.* **1929**, *51*, 2950−2964.
(43) Liu, Q.; Ma, L.; Li, K.; Wang, J.; Zang, Y. Apparent molar volumes of hydrophobic imidazolium type ionic liquids with dimethyl carbonate. *J. Mol. Liq.* **2020**, No. 113010.
(44) Millero, F. J. Molal volumes of electrolytes. *Chem. Rev.* **1971**, *71*, 147−176.
(45) Marcus, Y. Viscosity B-coefficients, structural entropies and heat capacities, and the effects of ions on the structure of water. *J. Solution Chem.* **1994**, *23*, 831−848.
(46) Tsangaris, J. M.; Martin, R. B. Viscosities of aqueous solutions of dipolar ions. *Arch. Biochem. Biophys.* **1965**, *112*, 267−272.
(47) Sarma, T.; Ahluwalia, J. Experimental studies on the structures of aqueous solutions of hydrophobic solutes. *Chem. Soc. Rev.* **1973**, *2*, 203−232.
(48) Glasstone, S.; Laidler, K. J.; Eyring, H. *The theory of rate processes*; McGraw-hill, 1941.
(49) Friedman, H.; Krishnan, C. Thermodynamics of ionic hydration. In *Aqueous Solutions of Simple Electrolytes*; Springer, 1973; pp. 1−118.
(50) Feakins, D.; Bates, F. M.; Waghorne, W. E.; Lawrence, K. G. Relative viscosities and quasi-thermodynamics of solutions of tert-butyl alcohol in the methanol−water system: a different view of the alkyl−water interaction. *J. Chem. Soc., Faraday Trans.* **1993**, *89*, 3381−3388.
(51) Feakins, D.; Freemantle, D. J.; Lawrence, K. G. Transition state treatment of the relative viscosity of electrolytic solutions. Applications to aqueous, non-aqueous and methanol+ water systems. *J. Chem. Soc., Faraday Trans.* **1974**, *70*, 795−806.
(52) Stokes, R. H.; Mills, R. Viscosity of electrolytes and related properties. *Am. J. Phys.* **1965**, *34*, 280.
(53) Friedman, H. L.; Krishnan, C. Studies of hydrophobic bonding in aqueous alcohols: enthalpy measurements and model calculations. *J. Solution Chem.* **1973**, *2*, 119−140.
(54) Dash, U.; Samantaray, B.; Mishra, S. Volumetric and viscometric studies of sodium nitroprusside in aqueous solutions at different temperatures. *J. Teach. Res. Chem.* **2005**, *11*, 87−90.
(55) Ghosh, B.; Sinha, A.; Roy, N.; Rajbanshi, B.; Mondal, M.; Roy, D.; Das, A.; Ghosh, N. N.; Dakua, V. K.; Roy, M. N. Molecular Interactions of Some Bioactive Molecules Prevalent in Aqueous Ionic Liquid Solutions at Different Temperatures Investigated by Experimental and Computational Contrivance. *Fluid Phase Equilib.* **2022**, No. 113415.
(56) Minkin, V. I. *Dipole moments in organic chemistry*; Springer Science & Business Media, 2012.
(57) Born, M.; Wolf, E. *Principles of optics: electromagnetic theory of propagation, interference and diffraction of light*; Elsevier, 2013.
(58) Deetlefs, M.; Seddon, K. R.; Shara, M. Predicting physical properties of ionic liquids. *Phys. Chem. Chem. Phys.* **2006**, *8*, 642−649.
(59) Bani-Yaseen, A. D.; Al-Rawashdeh, N.; Al-Momani, I. F. Influence of inclusion complexation with β-cyclodextrin on the photostability of selected imidazoline-derived drugs. *J. Incl. Phenom.* **2009**, *63*, 109−115.
(60) Caddeo, C.; Manconi, M.; Valenti, D.; Pini, E.; Sinico, C. Photostability and solubility improvement of β-cyclodextrin-included tretinoin. *J. Inclusion Phenom. Macrocyclic Chem.* **2007**, *59*, 293−300.
(61) Sirajuddin, M.; Ali, S.; Badshah, A. J. Drug−DNA interactions and their study by UV−Visible, fluorescence spectroscopies and cyclic voltametry. *Photochem. Photobiol. B.* **2013**, *124*, 1−19.
(62) Benesi, H. A.; Hildebrand, J. H. A spectrophotometric investigation of the interaction of iodine with aromatic hydrocarbons. *J. Am. Chem. Soc.* **1949**, *71*, 2703−2707.
(63) Arjmand, F.; Parveen, S.; Afzal, M.; Toupet, L.; Hadda, T. B. Molecular drug design, synthesis and crystal structure determination of CuII−SnIV heterobimetallic core: DNA binding and cleavage studies. *Eur. J. Med. Chem.* **2012**, *49*, 141−150.
(64) AL-Janabi, A. A. Treatment of Dermatophytoses by drugs containing some purine compounds. Ph. D. Thesis. AL-Mustansiryia Univ. College of science.(Arabic), 2004.
(65) Borkowski, A.; Ławniczak, Ł.; Cłapa, T.; Narożna, D.; Selwet, M.; Pęziak, D.; Markiewicz, B.; Chrzanowski, Ł. Different antibacterial activity of novel theophylline-based ionic liquids−Growth kinetic and cytotoxicity studies. *Ecotoxicol. Environ. Saf.* **2016**, *130*, 54−64.
(66) Carmona-Ribeiro, A. M.; de Melo Carrasco, L. D. Cationic antimicrobial polymers and their assemblies. *Int. J. Mol. Sci.* **2013**, *14*, 9906−9946.
(67) Ruddarraju, R. R.; Murugulla, A. C.; Kotla, R.; Tirumalasetty, M. C. B.; Wudayagiri, R.; Donthabakthuni, S.; Maroju, R.; Baburao, K.; Parasa, L. S. Design, synthesis, anticancer, antimicrobial activities and molecular docking studies of theophylline containing acetylenes and theophylline containing 1, 2, 3-triazoles with variant nucleoside derivatives. *Eur. J. Med. Chem.* **2016**, *123*, 379−396.
(68) Kim, H.; Yiluo, H.; Park, S.; Lee, J. Y.; Cho, E.; Jung, S. Characterization and enhanced antioxidant activity of the cysteinyl β-cyclodextrin-baicalein inclusion complex. *Molecules* **2016**, *21*, 703.
(69) Costa, P.; Medronho, B.; Gonçalves, S.; Romano, A. Products, Cyclodextrins enhance the antioxidant activity of essential oils from three Lamiaceae species. *Ind. Crops Prod.* **2015**, *70*, 341−346.

https://doi.org/10.1021/acsomega.2c01902
ACS Omega 2022, 7, 26211−26225